The Conformal Monogenic Signal of Image Sequences*

Lennart Wietzke[1], Gerald Sommer[1], Oliver Fleischmann[1], and Christian Schmaltz[2]

[1] Institute of Computer Science, Chair of Cognitive Systems, Christian-Albrechts-University, 24118 Kiel, Germany
[2] Mathematical Image Analysis Group, Faculty of Mathematics and Computer Science, Building E1 1, Saarland University, 66041 Saarbrücken, Germany

Summary. Based on the research results of the Kiel University Cognitive Systems Group in the field of multidimensional signal processing and Computer Vision, this book chapter presents new ideas in 2D/3D and multidimensional signal theory. The novel approach, called the *conformal monogenic signal*, is a rotationally invariant quadrature filter for extracting i(ntrinsic)1D and i2D *local* features of any curved 2D signal - such as lines, edges, corners and circles - without the use of any heuristics or steering techniques. The *conformal monogenic signal* contains the *monogenic signal* as a special case for i1D signals - such as lines and edges - and combines monogenic scale space, local energy, direction/orientation, both i1D and i2D phase and curvature in one unified algebraic framework. The *conformal monogenic signal* will be theoretically illustrated and motivated in detail by the relation of the 3D Radon transform and the generalized Hilbert transform on the sphere. The main idea of the *conformal monogenic signal* is to lift up 2D signals by *stereographic projection* to a higher dimensional conformal space where the local signal features can be analyzed with more degrees of freedom compared to the flat two-dimensional space of the original signal domain. The philosophy of the *conformal monogenic signal* is based on the idea to make use of the direct relation of the original two-dimensional signal and abstract geometric entities such as lines, circles, planes and spheres. Furthermore, the *conformal monogenic signal* can not only be extended to 3D signals (image sequences) but also to signals of any dimension.
The main advantages of the *conformal monogenic signal* in practical applications are the completeness with respect to the intrinsic dimension of the signal, the rotational invariance, the low computational time complexity, the easy implementation into existing Computer Vision software packages and the numerical robustness of calculating exact local curvature of signals without the need of any derivatives.

* We acknowledge funding by the German Research Foundation (DFG) under the projects *SO 320/4-2* and *We 2602/5-1*.

1 Introduction

Low level two-dimensional image analysis is often the first step of many Computer Vision tasks. Therefore, local signal features such as gray value or color information, gradient, curvature, orientation and phase determine the quality of subsequent higher level processing steps. It is important not to lose or to merge any of the original information within the local neighborhood of the test point[3]. The constraints of local signal analysis are: to span an orthogonal feature space (split of identity) and to be robust against stochastic and deterministic deviations between the actual signal and the model.
This book chapter is organized as follows: First the fundamental 1D and 2D local signal models with specific geometric and structural features are defined. The feature set of the assumed 2D signal model contains energy, phase, direction/orientation and curvature. Regarding those features, already known and closely related phase based and rotationally invariant quadrature filter signal processing approaches such as the monogenic signal, the structure multivector and the monogenic curvature tensor are being analyzed. Their possibilities and limitations are shown by means of the generalized Hilbert transform in Euclidean space and its relation to the Radon transform, which enables explicit extraction of the features by all different approaches in one framework. The monogenic signal, the structure multivector and the monogenic curvature tensor make use of generalized Hilbert transforms of different order in Euclidean space. Whereby the monogenic signal is limited to the first order generalized Hilbert transform and the structure multivector and the monogenic curvature tensor are extended to the second and third order generalized Hilbert transforms. The limitations of the nth-order generalized Hilbert transforms concerning 2D signal analysis are being shown and a novel 2D signal approach in conformal space called the *conformal monogenic signal* is presented.
Image signals $f \in L_2(\Omega;\mathbb{R})$ with $\Omega \subset \mathbb{R}^2$ will be locally analyzed on a low level. 2D signals are classified into local regions $N \subseteq \Omega$ of different intrinsic dimension (see figure 1)

$$\mathrm{i0D} = \{f \in L_2(\Omega;\mathbb{R}) : f(\mathbf{x}_i) = f(\mathbf{x}_j) \ \forall \mathbf{x}_i, \mathbf{x}_j \in N\} \tag{1}$$

$$\mathrm{i1D} = \{f \in L_2(\Omega;\mathbb{R}) : f(x,y) = g(x\cos\theta + y\sin\theta) \ \forall (x,y) \in N\} \setminus \mathrm{i0D} \tag{2}$$

$$\mathrm{i2D} = L_2(\Omega;\mathbb{R}) \setminus (\mathrm{i0D} \cup \mathrm{i1D}) \, . \tag{3}$$

The assumed local signal model is defined as a curve which can be locally approximated by a circle with arbitrary orientation and curvature

$$f(x,y) = a \ \cos\left(\left\| \begin{bmatrix} x \\ y \end{bmatrix} - \frac{1}{\kappa} \begin{bmatrix} \cos\theta \\ \sin\theta \end{bmatrix} \right\| + \phi\right) \in \mathrm{i1D} \cup \mathrm{i2D} \tag{4}$$

[3] There is no method of signal analysis which is universal in respect of any arbitrary local 2D structure. Hence, it is necessary to formulate a model of local signal structure as basis of the analysis. The great challenge is the search for a most general model which can cope with as much as possible variants of local signal structure.

with $a \in \mathbb{R}$ as the local amplitude, $\phi \in [0, 2\pi)$ as the local phase, $\kappa \in \mathbb{R}$ as the local curvature and $\theta \in [0, 2\pi)$ as the local direction/orientation of the signal for $\kappa \neq 0$. For the special case of $\kappa = 0$ the curved 2D signal degrades to an i1D function. Therefore the task is to solve an *inverse problem*, i.e. to determine local features such as amplitude a, phase ϕ, orientation θ and curvature κ of any curved signal such as lines, edges, corners and junctions. One important local structural feature is the phase ϕ which can be calculated by means of the Hilbert transform [10]. Furthermore all signals will be analyzed in *monogenic scale space* [7] since the Hilbert transform can only be interpreted for narrow banded signals

$$f(x, y; s_s) = \mathcal{P}(x, y; s_s) * f(x, y) \tag{5}$$

with $*$ as the convolution operator and s_s as the scale space parameter. The Poisson kernel of the applied low pass filter reads

$$\mathcal{P}(\mathbf{x}) = \mathcal{P}(\mathbf{x}; s_s) = \frac{s_s}{2\pi \left(s_s^2 + \|\mathbf{x}\|^2\right)^{\frac{n+1}{2}}}, \quad n \in \mathbb{N},\ \mathbf{x} \in \mathbb{R}^n\ . \tag{6}$$

Fig. 1. From left to right: a constant signal (i0D), an arbitrary rotated 1D signal (i1D) and an i2D checkerboard signal consisting of two simple superimposed i1D signals. A curved i2D signal and two superimposed curved i2D signals. Note that all signals displayed here preserve their intrinsic dimension globally.

1.1 Related Work

Phase and energy of 1D signals can be analyzed by the *analytic signal* [10]. The generalization of the analytic signal to multidimensional signal domains has been done by the *monogenic signal* [6]. In case of 2D signals the *monogenic signal* delivers local phase, orientation and energy information restricted to the set of i1D signals. This book chapter presents the generalization of the *monogenic signal* for 2D signals to analyze both i1D and i2D signals in one unified framework. The *conformal monogenic signal* delivers local phase, orientation, energy and curvature for i1D and i2D signals with the *monogenic signal* as a special case. The *monogenic signal* replaces the classical 1D Hilbert transform of the analytic signal by the generalized Hilbert transform [3]

$$R\{f\}(\mathbf{x}) = (\mathcal{Q} * f)(\mathbf{x}) = (h_n * \mathcal{P} * f)(\mathbf{x}), \quad \mathbf{x} \in \mathbb{R}^n,\ n \in \mathbb{N} \setminus \{1\} \tag{7}$$

with $\mathcal{Q}$ as the conjugate Poisson kernel and h_n as the generalized Hilbert transform kernel

$$h_n(\mathbf{x}) = \frac{2}{A_{n+1}} \frac{\mathbf{x}}{\|\mathbf{x}\|^{n+1}}, \quad \mathbf{x} \in \mathbb{R}^n,\ n \in \mathbb{N} \setminus \{1\} \tag{8}$$

with A_{n+1} as the surface area of the unit sphere $\mathbb{S}^n$ in Euclidian space $\mathbb{R}^{n+1}$. To enable interpretation of the generalized Hilbert transform, its relation to the Radon transform is the key [20]. The generalized Hilbert transform can be expressed by a concatenation of the Radon transform, the inverse Radon transform and the well known classical 1D Hilbert transform. Note that the relation to the Radon transform is required solely for interpretation and theoretical results. Neither the Radon transform nor its inverse are ever applied to the signal in practice. Instead the generalized Hilbert transformed signal will be determined by convolution in spatial domain and the signal features can be extracted in a rotationally invariant way.

2 Generalized Hilbert Transforms in Conformal Space

The feature space of the 2D *monogenic signal* is spanned by phase, orientation and energy information. This restriction correlates to the dimension of the associated 2D Radon space [20]. Therefore, our main idea is that the feature space of the 2D signal can only be extended by lifting up the original signal to higher dimensions. This is one of the main ideas of the *conformal monogenic signal*. In the following the 2D monogenic signal will be generalized to analyze also i2D signals by embedding the 2D signal into the 3D conformal space [15]. The 2D generalized Hilbert transform can be expressed by the 2D Radon transform which integrates all function values on lines [17]. This restriction to lines is one of the reasons why the 2D monogenic signal is limited to i1D signals (such as lines and edges) and can not be applied to corners and general curves. To analyze also i2D signals and to measure curvature $\kappa = \frac{1}{\rho}$, a 2D Radon transform which integrates on curved lines (i.e. local circles with radius ρ) is preferable. In the 3D domain the Radon transform integrates on planes, although at first sight 3D planes are not related to 2D signals. But the idea is that circles form the intersection of a sphere (with center at $\left[0, 0, \frac{1}{2}\right]$ and radius $\rho = \frac{1}{2}$) and planes passing through the origin $(0, 0, 0)$ of 3D space. Since the generalized Hilbert transform can be extended to any dimension [4] and the 3D generalized Hilbert transform can be expressed by the 3D Radon transform, the 2D signal coordinates must be mapped appropriately to the sphere. This mapping must be conformal (i.e. angle preserving), so that angular feature interpretation of the 3D generalized Hilbert transform in conformal space is still reasonable. Analogous to the line parametrization by $(t, \theta) \in \mathbb{R} \times [0, \pi)$ (where $t \in \mathbb{R}$ is the minimal distance of the 2D line to the origin and $\theta \in [0, \pi)$ is the orientation of the line) of the 2D Radon transform [20], the planes of the 3D Radon transform are uniquely defined by the parameters $(t, \theta, \varphi) \in$

$\mathbb{R} \times [0, 2\pi) \times [0, \pi)$ where t is the minimal distance of the plane to the origin of the 3D space and the angles θ and φ determine the orientation of the plane in 3D space (see figure 3). This new parametrization truly extends the interpretation space of the monogenic signal by one dimension. In contrast to the well known Monge patch embedding known from differential geometry [5], the original 2D signal will now be embedded into the conformal space.

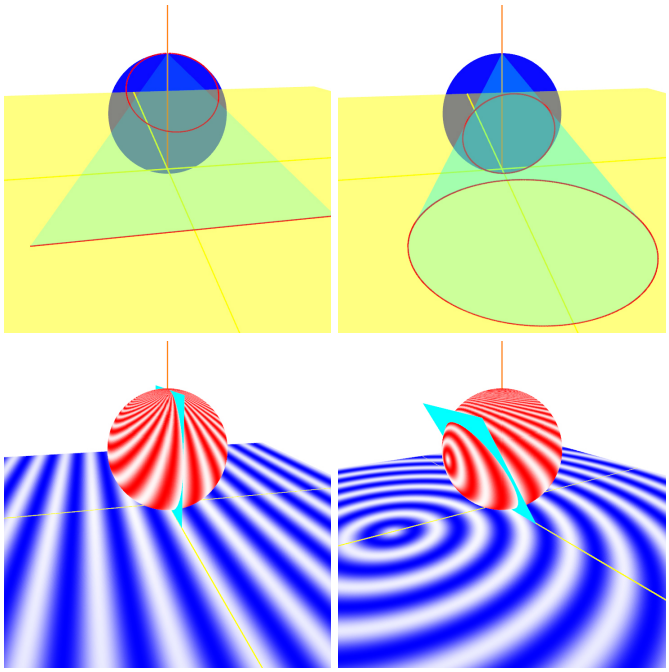

Fig. 2. Lines and circles of the 2D image domain are both mapped to circles on the sphere. Each circle on the sphere is uniquely defined by its parameterized intersection plane in conformal space. The third figure illustrates the monogenic signal as a special case.

2.1 The Conformal Space

The main idea is that the concept of lines in 2D Radon space becomes the concept of planes in 3D Radon space and the more abstract concept of hyperplanes in multidimensional space. These planes determine circles on the sphere in conformal space. Since lines and circles of the 2D signal domain are mapped to circles [15] on the sphere (see figure 2), the integration on these circles determines points in the 3D Radon space. The projection $\mathcal{C}$ known from complex analysis [15] maps the original 2D signal domain to the sphere and can be inverted by $\mathcal{C}^{-1}$

$$\mathcal{C}(x,y) = \frac{1}{x^2+y^2+1}\begin{bmatrix} x \\ y \\ x^2+y^2 \end{bmatrix}, \quad \mathcal{C}^{-1}(\xi_1,\xi_2,\xi_3) = \frac{1}{1-\xi_3}\begin{bmatrix} \xi_1 \\ \xi_2 \end{bmatrix}. \tag{9}$$

This mapping has the property that the 2D origin $(0,0)$ of a local coordinate system will be mapped to the south pole $(0,0,0)$ of the sphere in conformal space and both $-\infty, +\infty$ will be mapped to the north pole $(0,0,1)$ of the sphere. Lines and circles of the 2D signal domain will be mapped to circles on the sphere and can be determined uniquely by planes in 3D conformal space. The integration on these planes corresponds to points (t,θ,φ) in the 3D Radon space.

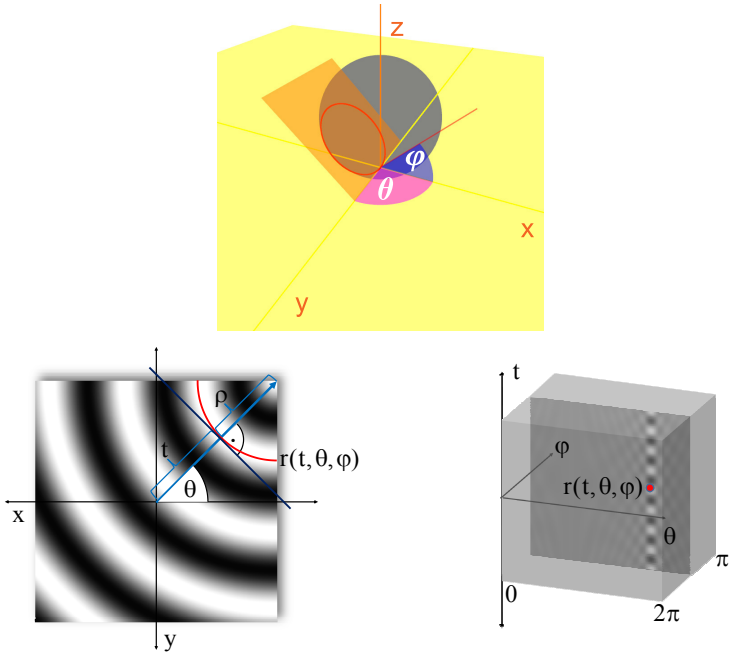

Fig. 3. Top row: Each with the triple (t,θ,φ) with $t=0$ parameterized plane can be determined exactly by the generalized Hilbert transforms on the sphere. The interpretation of this parameter set delivers the features such as direction, phase and curvature of the original signal without any steering. Bottom row left figure: Curved i2D signal with orientation θ and curvature $\kappa = \frac{1}{\rho}$. Bottom row right figure: Corresponding 3D Radon space representation of the i2D signal spanned by the parameters t, θ and φ. Since the Radon transform on circles directly on the plane of the original 2D signal is not possible, the Radon transform has to be done in higher dimensional 3D conformal space where circles correspond to planes.

2.2 3D Radon Transform in Conformal Space

To interpret the *conformal monogenic signal*, the relation to the 3D Radon transform in conformal space must be taken into account. The 3D Radon transform is defined as the integral of all function values on the plane (see figure 2) defined by

$$\mathcal{R}\left\{c\right\}(t,\theta,\varphi) = \int\limits_{\mathbf{x}\in\mathbb{R}^3} c(\mathbf{x})\delta_0(\mathbf{x}\begin{bmatrix}\sin\varphi\cos\theta\\ \sin\varphi\sin\theta\\ \cos\varphi\end{bmatrix} - t)d\mathbf{x} \tag{10}$$

with δ_0 as the Dirac distribution and the mapping c defined in equation (12). Since the signal is mapped on the sphere and all other points of the conformal space are set to zero, the 3D Radon transform actually sums up all points lying on the intersection of the plane and the sphere. For all planes this intersection can either be empty or a circle. The concept of circles in the conformal 3D Radon transform can be compared with the concept of lines known from the 2D Radon transform. Since lines in the 2D signal domain are also mapped to circles, the *conformal monogenic signal* can analyze i1D as well as curved i2D signals in one single framework. Recall the very important fact that every corner or curve can be locally approximated by a circle. The inverse 3D Radon transform exists and differs from the 2D case such that it is a *local* transformation [2].

$$\mathcal{R}^{-1}\{r\}(0,0,0) = -\frac{1}{8\pi^2}\int\limits_{\theta=0}^{2\pi}\int\limits_{\varphi=0}^{\pi}\frac{\partial^2}{\partial t^2}\, r(t,\theta,\varphi)|_{t=0}\, d\varphi\, d\theta\,. \tag{11}$$

That means the generalized Hilbert transform at $(0,0,0)$ is completely determined by all planes passing the origin (i.e. $t = 0$). In contrast, the 2D monogenic signal requires all integrals on all lines (t,θ) to reconstruct the original signal at a certain point and is therefore called a *global* transform. This interesting fact turns out from the definition of the inverse 3D Radon transform $\mathcal{R}^{-1}\{\cdot\}$. Therefore, the local features of i1D and i2D signals can be determined by the *conformal monogenic signal* at each test point of the original 2D signal without knowledge of the whole 3D Radon space.

2.3 The 2D Conformal Monogenic Signal

To give the generalized Hilbert transform more degrees of freedom for signal analysis, the original 2D signal will be embedded in a applicable subspace of the 3D conformal space by the mapping

$$c(x,y,z) = \begin{cases} f(\mathcal{C}^{-1}(x,y,z)^T; s_s) & , x^2+y^2+\left(z-\frac{1}{2}\right)^2 = \frac{1}{4} \\ 0 & , \text{else} \end{cases}\,. \tag{12}$$

Thus, the 3D generalized Hilbert transform can be applied to all points on the sphere. The center of convolution in spatial domain is the south pole $(0,0,0)$ where the test point of the 2D signal domain meets the sphere. At this point the 3D generalized Hilbert transform will be performed at the origin ($\mathbf{0}$) of the applied local coordinate system for each test point separately. The *conformal monogenic signal* [19, 18] is defined as

$$f_{\mathrm{CMS}}(\mathbf{0}) = \left[c(\mathbf{0}), R_x\left\{c\right\}(\mathbf{0}), R_y\left\{c\right\}(\mathbf{0}), R_z\left\{c\right\}(\mathbf{0})\right]^T \tag{13}$$

and can be expressed by the classical 1D Hilbert transform kernel $h_1(\tau) = \frac{1}{\pi\tau}$ [10], the 3D Radon transform and its inverse analogous to the monogenic signal in 2D [20]

$$\begin{bmatrix} R_x\left\{c\right\}(\mathbf{0}) \\ R_y\left\{c\right\}(\mathbf{0}) \\ R_z\left\{c\right\}(\mathbf{0}) \end{bmatrix} = \left[\mathcal{R}^{-1}\left\{ \begin{bmatrix} \sin\varphi\cos\theta \\ \sin\varphi\sin\theta \\ \cos\varphi \end{bmatrix} h_1(t) * \mathcal{R}\left\{c\right\}(t,\theta,\varphi) \right\}(0,0,0) \right] \tag{14}$$

with $*$ as the 1D convolution operator. Compared to the 2D monogenic signal the *conformal monogenic signal* performs a 3D generalized Hilbert transformation in conformal space.

2.4 Interpretation

Analogous to the interpretation of the *monogenic signal* in [20], the parameters of the plane within the 3D Radon space determine the local features of the curved i2D signal (see figure 2). The *conformal monogenic signal* can be called the generalized monogenic signal for i1D and i2D signals, because the special case of lines and edges can be considered as circles with zero curvature. These lines are mapped to circles passing through the north pole in conformal space. The parameter θ will be interpreted as the orientation in i1D case and naturally deploys to direction $\theta \in [0, 2\pi)$ for the i2D case

$$\theta = \operatorname{atan2}\left(R_y\left\{c\right\}(\mathbf{0}), R_x\left\{c\right\}(\mathbf{0})\right) \ . \tag{15}$$

The energy of the signal is defined by

$$E = a^2 = c^2(\mathbf{0}) + R_x^2\left\{c\right\}(\mathbf{0}) + R_y^2\left\{c\right\}(\mathbf{0}) + R_z^2\left\{c\right\}(\mathbf{0}) \ . \tag{16}$$

The i1D and i2D curvature phase is defined by

$$\phi = \operatorname{atan2}\left(\sqrt{R_x^2\left\{c\right\}(\mathbf{0}) + R_y^2\left\{c\right\}(\mathbf{0}) + R_z^2\left\{c\right\}(\mathbf{0})}, c(\mathbf{0})\right) \ . \tag{17}$$

Note that all proofs are analogous to those for the 2D monogenic signal shown in [20].

2.5 Local Curvature

The parameter φ of the 3D Radon space corresponds to the isophote curvature κ [14] known from differential geometry

$$\varphi = \arctan \frac{\sqrt{R_x^2\{c\}(\mathbf{0}) + R_y^2\{c\}(\mathbf{0})}}{R_z\{c\}(\mathbf{0})} \tag{18}$$

$$\kappa = \frac{-f_{xx}f_y^2 + 2f_x f_y f_{xy} - f_{yy}f_x^2}{\left(f_x^2 + f_y^2\right)^{\frac{3}{2}}} \tag{19}$$

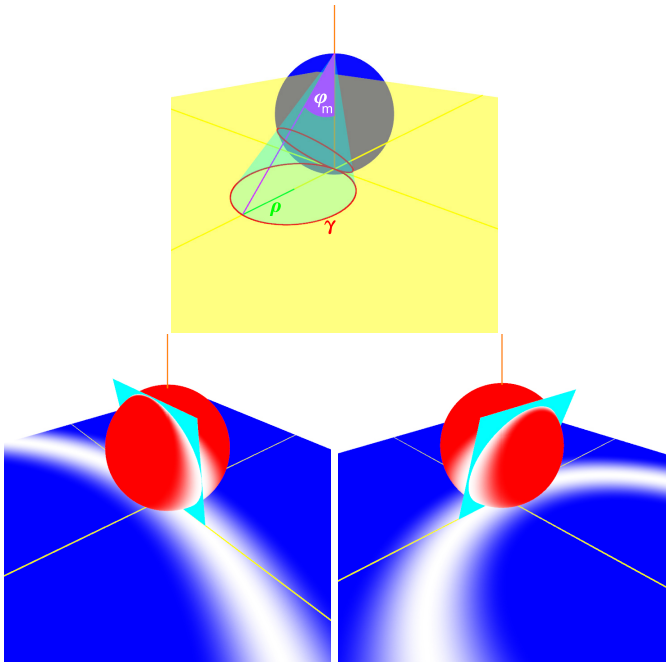

Fig. 4. Top row: Visualization of the circle described by γ projected to $\mathbb{S}^2(m_S, \rho_S)$. This figure illustrates geometrically the relation of the curvature κ to the orientation parameter φ of the hyperplane in 3D Radon space $\frac{1}{\kappa} = \rho = \tan\varphi_m$.

Proof:
Let be

$$\gamma(t) = [\rho(\cos\theta + \cos t), \rho(\sin\theta + \sin t)]^T \tag{20}$$

with $t \in [0, 2\pi)$ a parametrization of a circle in the 2D plane touching the origin $(0, 0)$ with radius ρ and tangential orientation θ. This circle will be the

model for the osculating circle touching the isophote curve of the 2D signal f at the origin $(0,0)$ of the local coordinate system for each test point. Therefore,

$$f(\gamma(t_1)) = f(\gamma(t_2)) \; \forall t_1, t_2 \in [0, 2\pi) \; . \tag{21}$$

Define $\gamma_S(t) = \mathcal{C}(\gamma(t))$ as the projection of γ to the sphere

$$\mathbb{S}^2(m_S, \rho_S) = \left\{ v \in \mathbb{R}^3 : \|v - m_S\| = \rho_S \right\} \tag{22}$$

with the center $m_S = \left[0, 0, \frac{1}{2}\right]^T$ and the radius $\rho_S = \frac{1}{2}$. Furthermore define

$$f_S(\gamma_S(t)) = f(\mathcal{C}^{-1}(\gamma_S(t))) \; . \tag{23}$$

The conjugate Poisson kernel in $\mathbb{R}^{n+1}_+$ reads

$$\mathcal{Q}(x) = [\mathcal{Q}_x(x), \mathcal{Q}_y(x), \mathcal{Q}_z(x)]^T = (h_3 * \mathcal{P})(x) \tag{24}$$

with

$$R\{f_S\}(\mathbf{x}) = (\mathcal{Q} * f_S)(\mathbf{x}) \; . \tag{25}$$

The radius ρ of the osculating circle described by the parameterized curve γ reads

$$\rho = \frac{2R_z\{f_S\}(\mathbf{0})}{\sqrt{R_x^2\{f_S\}(\mathbf{0}) + R_y^2\{f_S\}(\mathbf{0})}} \; . \tag{26}$$

Since the values of $f_S(x)$ will only be nonzero for $x \in \mathbb{S}^2(m_S, \rho_S)$, the integration can be restricted to the ball

$$\mathbb{B}^2(m_S, \rho_S) = \left\{ v \in \mathbb{R}^3 : \|v - m_S\| \leqslant \rho_S \right\} \; . \tag{27}$$

Furthermore $f_S(x)$ is only nonzero for the circle projected on the sphere

$$M = \{\gamma_S(t) : t \in [0, 2\pi)\} \; . \tag{28}$$

Now let $\mathbb{S}^2(m, \rho)$ be the sphere whose intersection with $\mathbb{S}^2(m_S, \rho_S)$ results in M. Then the set M is a circle on the surface of both $\mathbb{S}^2(m_S, \rho_S)$ and $\mathbb{S}^2(m, \rho)$. The integration over the volumes of $\mathbb{B}^2(m, \rho)$ and $\mathbb{B}^2(m_S, \rho_S)$ will be the same.

$$\int\limits_{x \in \mathbb{R}^3_+} \mathcal{Q}(x) f_S(x) \; dx = \int\limits_{x \in \mathbb{B}^2(m_S, \rho_S)} \mathcal{Q}(x) f_S(x) \; dx = \int\limits_{x \in \mathbb{B}^2(m, \rho)} \mathcal{Q}(x) f_S(x) \; dx \tag{29}$$

According to the results from harmonic analysis [1] the convolution of a function in $\mathbb{R}^n$ with the Poisson kernel $\mathcal{P}$ in upper the half space $\mathbb{R}^{n+1}_+$ results in a harmonic function in $\mathbb{R}^{n+1}_+$. Therefore, $\mathcal{Q}$ is harmonic in $\mathbb{R}^{3+1}_+$. Using the *mean value theorem* for harmonic functions it follows that

$$\int\limits_{x \in \mathbb{B}^2(m, \rho)} \mathcal{Q}(x) \; dx = k \; \mathcal{Q}(m) \tag{30}$$

with the components of $\mathcal{Q}$ written in spherical coordinates

$$\mathcal{Q}(m) = \begin{bmatrix} \mathcal{Q}_x(m) \\ \mathcal{Q}_y(m) \\ \mathcal{Q}_z(m) \end{bmatrix} = \frac{1}{\left[\|m\|^2 + s_s^2\right]^2} \begin{bmatrix} \sin\varphi_m \cos\theta_m \\ \sin\varphi_m \sin\theta_m \\ \cos\varphi_m \end{bmatrix} \tag{31}$$

with s_s as the scale space parameter. Since f_S is the signal model for the isophote curve of a signal in the plane, it is a curve consisting of constant values. Therefore, $f_S(x)$ will be constant for all $x \in M$ which results in

$$\int\limits_{x \in \mathbb{B}^2(m,\rho)} \mathcal{Q}(x) f_S(x)\, dx = f_c \int\limits_{x \in \mathbb{B}^2(m,\rho)} \mathcal{Q}(x)\, dx = f_c\, k\, \mathcal{Q}(m)\,. \tag{32}$$

With equation (26) it is now possible to determine $\frac{\sin\varphi_m}{\cos\varphi_m}$. Figure 4 illustrates that this is exactly $\frac{\rho}{2\,\rho_S}$. Since $\rho_S = \frac{1}{2}$ it follows that the radius of the local curvature can be determined by

$$\rho = \frac{\sin\varphi_m}{2\cos\varphi_m} = \frac{\sqrt{\mathcal{Q}_x^2(m) + \mathcal{Q}_y^2(m)}}{2\mathcal{Q}_z(m)}\,. \tag{33}$$

2.6 Phase Congruency of the Conformal Monogenic Signal

Since the local phase of the *conformal monogenic signal* is independent of the local signal amplitude a_{s_s}, it thus has the advantage of being not sensitive to local illumination changes. Hence, detecting i1D and i2D key points can be done by searching for points of *stationary phase* [12, 11, 16, 21] in monogenic scale-space. This approach is called *phase congruency* ϕ_{PC} and is based on comparisons of the local phase at certain distinct scales $s_s > 0$

$$\phi_{\mathrm{PC}} = \frac{\sum\limits_{s_s \in I} W \left\lfloor a_{s_s}(\cos(\phi_{s_s} - \overline{\phi}) - \|\sin(\phi_{s_s} - \overline{\phi})\| - T)\right\rfloor}{\varepsilon + \sum\limits_{s_s \in I} a_{s_s}} \tag{34}$$

with s_s as the scale-space parameter within the interval $I \subset [s_f, \cdots, s_c]$ with $\|I\| \in \mathbb{N}, W \in \mathbb{R}$ as a weighting factor for frequency spread. $a_{s_s}^2 = e_{s_s} = e = a^2$ is the local signal amplitude of the *conformal monogenic signal* at the scale-space parameter s_s and ϕ_{s_s} is the local phase of the *conformal monogenic signal* at the scale-space parameter s_s. $\overline{\phi} = \frac{1}{\|I\|} \sum_{s_s \in I} \phi_{s_s}$ is the mean local phase for all scale-space parameters $s_s \in I$ and ε is a constant because of numerical reasons to avoid division by zero,

$$\lfloor x \rfloor = \begin{cases} x, & x > 0 \\ 0, & \text{else} \end{cases} \tag{35}$$

The estimated noise influence value T is a constant to ensure that only energy values that exceed T are taken into account. The phase congruency measure

can be directly applied to detect rotationally invariant i1D and i2D image structures. Any test point with a phase congruency greater than a certain threshold can be marked as a i1D or i2D point respectively.
The so far discussed phase congruency approach is based on comparisons of local phase at certain distinct scales. Nevertheless, there exist some drawbacks. Since local features are relatively to the scale, an algorithm using distinct scales has to contain heuristics to judge whether the structure is present or not if the phase is only congruent in some of the considered scales. Besides, it is not straightforward, how to map at different scales estimated phases to a certainty measure. Hence, the *differential phase congruency* [7] detects i1D and i2D structures in a more simple and efficient way. The points in monogenic scale-space, where the differentials of their phase vector $\Phi(s_s)$ are zero, are called points of differential phase congruency. They have to be identified as i1D or i2D structures. The scale derivative of the phase vector reads

$$\frac{\partial}{\partial s_s}\Phi(s_s) = \frac{c(\mathbf{0};s_s)\begin{bmatrix}\frac{\partial}{\partial s_s}R_x\{c\}(\mathbf{0};s_s)\\ \frac{\partial}{\partial s_s}R_y\{c\}(\mathbf{0};s_s)\\ \frac{\partial}{\partial s_s}R_z\{c\}(\mathbf{0};s_s)\end{bmatrix} - \frac{\partial}{\partial s_s}c(\mathbf{0};s_s)\begin{bmatrix}R_x\{c\}(\mathbf{0};s_s)\\ R_y\{c\}(\mathbf{0};s_s)\\ R_z\{c\}(\mathbf{0};s_s)\end{bmatrix}}{c(\mathbf{0},s_s)^2 + \left\|R\{c\}(\mathbf{0};s_s)\right\|^2} \tag{36}$$

Test points where $\frac{\partial}{\partial s_s}\Phi(s_s) = 0$ are of differential phase congruency and hence considered as i1D or i2D structures. To find these points, the zeros of the three components of the numerator in equation (36) have to be found. These zeros can be easily obtained with subpixel accuracy by a *linear regression*. The differential phase congruency is quite useful since it yields a higher accuracy and a significant speedup of the derivative computation compared to a finite difference approximation.

2.7 Experimental Results

On synthetic signals with known ground truth the average error of the feature extraction converges to zero with increasing refinement of the convolution mask size. Under the presence of noise the *conformal monogenic signal* curvature performs more robust than e.g. the gradient based Sobel detector (see figure 5). The curvature feature delivered by the novel *conformal monogenic signal* performs better in dense optical flow applications with an average angular error (AAE) of 1.99° compared to [22] (with $AAE = 2.67°$) on the cloudy Yosemite sequence (see figure 5). Since the *conformal monogenic signal* combines all intrinsic dimensions in one framework it could be an interesting alternative for the gradient or the Laplace operator.

3 The 3D Conformal Monogenic Signal

In case of *visual motion analysis* a three dimensional isotropic quadrature filter is needed [13, 8]. The *conformal monogenic signal* of a 3D signal $f \in$

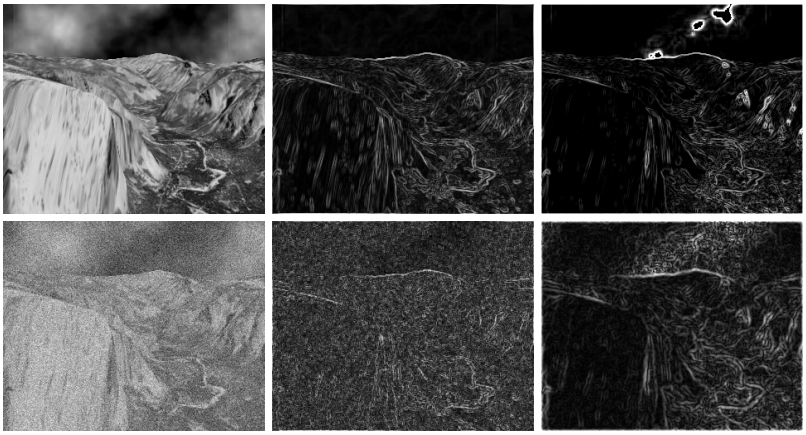

Fig. 5. Top row from left to right: Original Yosemite image, Sobel detector output and *conformal monogenic signal* curvature which delivers much more structural information (see cloudy sky). Bottom row from left to right: Noise degraded image (SNR=10dB), blurred Sobel output and *conformal monogenic signal* curvature. Convolution mask size: 7×7 pixels.

$L_2(\Omega;\mathbb{R})$ with $\Omega \subset \mathbb{R}^3$ delivers energy, 3D orientation, phase and curvature. For image sequences (3D signals) the concept of planes in 3D Radon space becomes the more abstract concept of hyperplanes in 4D Radon space. These 4D hyperplanes determine 3D spheres on the 4D hypersphere in 4D conformal space. Since 3D planes and 3D spheres of the three-dimensional signal domain are mapped to 3D spheres on the 4D hypersphere, the integration on these 3D spheres determines points in the 4D Radon space. The general stereographic projection for any dimension $n \in \mathbb{N}$ which maps the Euclidian space $\mathbb{R}^n$ to the conformal space $\mathbb{R}^{n+1}$ reads

$$\mathcal{C}(x_1, x_2, \cdots, x_n) = \frac{1}{1+\sum_{i=1}^{n} x_i^2} \begin{bmatrix} x_1 \\ x_2 \\ \cdots \\ x_n \\ \sum_{i=1}^{n} x_i^2 \end{bmatrix} \in \mathbb{R}^{n+1} \,. \tag{37}$$

The stereographic projection maps the Euclidian space $\mathbb{R}^n$ to the hypersphere in $\mathbb{R}^{n+1}$ with radius $\frac{1}{2}$ and the south pole of the hypersphere touching the origin $(\underbrace{0, \cdots, 0}_{n}) \in \mathbb{R}^n$ of the Euclidian space $\mathbb{R}^n$ and the north pole of the hypersphere with coordinates $(\underbrace{0, 0, \cdots, 0}_{n}, 1) \in \mathbb{R}^{n+1}$. For the signal dimension $n = 3$ the stereographic projection $\mathcal{C}$ known from complex analysis [9] maps the 3D signal domain to the hypersphere

$$\mathcal{C}(x,y,z) = \frac{1}{1+x^2+y^2+z^2}\begin{bmatrix} x \\ y \\ z \\ x^2+y^2+z^2 \end{bmatrix}. \tag{38}$$

This projection is conformal and can be inverted by the general formula

$$\mathcal{C}^{-1}(\xi_1,\xi_2,\cdots,\xi_n,\xi_{n+1}) = \frac{1}{1-\xi_{n+1}}\begin{bmatrix} \xi_1 \\ \xi_2 \\ \cdots \\ \xi_n \end{bmatrix}. \tag{39}$$

The inversion $\mathcal{C}^{-1}$ for all elements of the hypersphere reads

$$\mathcal{C}^{-1}(\xi_1,\xi_2,\xi_3,\xi_4) = \frac{1}{1-\xi_4}\begin{bmatrix} \xi_1 \\ \xi_2 \\ \xi_3 \end{bmatrix} \tag{40}$$

with $\xi = (\xi_1,\xi_2,\xi_3,\xi_4)$. This mapping has the property that the origin $(0,0,0)$ of the 3D signal domain will be mapped to the south pole $\mathbf{0} = (0,0,0,0)$ of the hypersphere and both $-\infty, +\infty$ will be mapped to the north pole $(0,0,0,1)$ of the hypersphere. 3D planes and spheres of the 3D signal domain will be mapped to spheres on the hypersphere and can be determined uniquely by hyperplanes in 4D Radon space. The integration on these hyperplanes corresponds to points $(t,\theta_1,\theta_2,\varphi)$ in the 4D Radon space.
Since the signal domain $\Omega \subset \mathbb{R}^3$ is bounded, not the whole hypersphere is covered by the original signal. Anyway, all hyperplanes corresponding to spheres on the hypersphere remain unchanged. That is the reason why the *conformal monogenic signal* models 3D planes and all kinds of curved 3D planes which can be locally approximated by spheres. To give the Riesz transform more degrees of freedom, the original three-dimensional signal will be embedded in an applicable subspace of the conformal space by the so called *conformal signal* $c \in \mathbb{R}^{(\mathbb{R}^4)}$ of the original 3D signal f:

$$c(\xi) = \begin{cases} f(\mathcal{C}^{-1}(\xi_1,\xi_2,\xi_3,\xi_4)^T) & ,\xi_1^2+\xi_2^2+\xi_3^2+\left(\xi_4-\frac{1}{2}\right)^2 = \frac{1}{4} \\ 0 & ,\text{else} \end{cases} \tag{41}$$

Thus, the 4D Riesz transform $R\{\cdot\}$ can be applied to all points on the hypersphere. The center of convolution in spatial domain is the south pole $(0,0,0,0)$ where the origin of the 3D signal domain meets the hypersphere. At this point the 4D Riesz transform $R\{\cdot\}(\mathbf{0})$ will be evaluated in spatial domain by convolution

$$R\{c\}(\xi)|_{\xi=(0,0,0,0)} = \frac{2}{A_5}\text{P.V.}\int\limits_{x\in\mathbb{R}^4} \frac{x}{\|x\|^5}\, c(x-\xi)\, dx \tag{42}$$

with P.V. as the Cauchy principal value and A_5 as the surface area of the unit sphere $\mathbb{S}^4$. The *conformal monogenic signal* f_{CM} for 3D signals is defined by

the even part and the four odd parts of the 4D Riesz transform in conformal space

$$f_{\mathrm{CM}}(0,0,0) = \begin{bmatrix} c_e(\mathbf{0}) \\ c_{o_1}(\mathbf{0}) \\ c_{o_2}(\mathbf{0}) \\ c_{o_3}(\mathbf{0}) \\ c_{o_4}(\mathbf{0}) \end{bmatrix} = \begin{bmatrix} c(\mathbf{0}) \\ R_1\{c\}(\mathbf{0}) \\ R_2\{c\}(\mathbf{0}) \\ R_3\{c\}(\mathbf{0}) \\ R_4\{c\}(\mathbf{0}) \end{bmatrix} = \begin{bmatrix} c(\mathbf{0}) \\ R\{c\}(\mathbf{0}) \end{bmatrix} . \tag{43}$$

Note that the coordinates $(0,0,0)$ are relative to the local coordinate system for each test point of the original 3D signal and $\mathbf{0} = (0,0,0,0)$ are the corresponding relative coordinates in conformal space, i.e. this is no restriction.
The Riesz transform of the 3D signal embedded in the conformal space can also be written in terms of the 4D Radon transform and its inverse

$$R\{c\}(\mathbf{0}) = \mathcal{R}^{-1}\left\{ \begin{bmatrix} \cos\varphi \sin\theta_1 \sin\theta_2 \\ \sin\varphi \sin\theta_1 \sin\theta_2 \\ \cos\theta_1 \sin\theta_2 \\ \cos\theta_2 \end{bmatrix} h_1(t) * \mathcal{R}\{c\}(t,\theta_1,\theta_2,\varphi) \right\}(\mathbf{0}) . \tag{44}$$

This representation of the Riesz transform is essential for the subsequent interpretation of the *conformal monogenic signal*. Remember that without loss of generality the signal will be analyzed at the origin $\mathbf{0} = (0,0,0)$ of the local coordinate system of the test point of local interest. Compared to the 2D monogenic signal the *conformal monogenic signal* of 3D signals is based on a 4D Riesz transformation in conformal space.
Analogous to the interpretation of the monogenic signal in [20], the parameters of the hyperplane within the 4D Radon space determine the local features of the curved 3D signal. The norm of the 4D Riesz transform of the *conformal signal* is defined by

$$\|R\{c\}(\mathbf{0})\| = \sqrt{R_1^2\{c\}(\mathbf{0}) + R_2^2\{c\}(\mathbf{0}) + R_3^2\{c\}(\mathbf{0}) + R_4^2\{c\}(\mathbf{0})} . \tag{45}$$

The *conformal monogenic signal* can be called the generalized monogenic signal for 3D signals, because the special case of planes in the original 3D signal can be considered as spheres with zero curvature. These planes are mapped to spheres passing through the north pole in conformal space. The 3D curvature corresponds to the parameter φ of the 4D Radon space,

$$\varphi = \arctan \frac{R_2^2\{c\}(\mathbf{0})}{R_1^2\{c\}(\mathbf{0})} . \tag{46}$$

Besides, the curvature of the *conformal monogenic signal* naturally indicates the intrinsic dimension of the signal. The parameters (θ_1, θ_2) will be interpreted as the orientation of the signal in the original 3D space

$$\theta_1 = \arcsin \frac{\sqrt{R_1^2\{c\}(\mathbf{0}) + R_2^2\{c\}(\mathbf{0})}}{R_4\{c\}(\mathbf{0})} \tag{47}$$

and

$$\theta_2 = \operatorname{atan2}\left(\sqrt{R_1^2\left\{c\right\}\left(\mathbf{0}\right) + R_2^2\left\{c\right\}\left(\mathbf{0}\right) + R_3^2\left\{c\right\}\left(\mathbf{0}\right)}, R_4\left\{c\right\}\left(\mathbf{0}\right)\right) \ . \tag{48}$$

The energy of the signal is defined by

$$e = c^2(\mathbf{0}) + \left\|R\left\{c\right\}\left(\mathbf{0}\right)\right\|^2 \ . \tag{49}$$

The phase for curved 3D signals is defined by

$$\phi = \operatorname{atan2}\left(\left\|R\left\{c\right\}\left(\mathbf{0}\right)\right\|, c(\mathbf{0})\right) \ . \tag{50}$$

In all different intrinsic dimensions the phase indicates a measure of parity symmetry. Note that all proofs are analogous to those for the 2D monogenic signal shown in [20].

3.1 Implementation

The implementation of the *conformal monogenic signal* of 3D signals such as images sequences is analogous to the 2D signal case. The computational time complexity is in $O(n^3)$ with n as the convolution mask size in one dimension.

```
//Input:  double Image3D(double x,double y,double z)
//Input:  double x,y,z (Local pixel test point for analysis)
//Input:  double Coarse > Fine > 0 (Bandpass filter parameters)
//Input:  double Size > 0 (Convolution mask size)
//Output: Direction1, Direction2, Phase, Curvature, Energy

double Coarse=2,Fine=0.1; int Size=5;//e.g.
double rp=0,r1=0,r2=0,r3=0,r4=0;
for(double cx = -Size;cx <= Size;cx += 1)
for(double cy = -Size;cy <= Size;cy += 1)
for(double cz = -Size;cz <= Size;cz += 1)
{
    //Map points (cx,cy,cz) to conformal space (x1,x2,x3,x4)
    double d = pow(cx,2)+pow(cy,2)+pow(cz,2)+1;
    double x1 = cx    / d;
    double x2 = cy    / d;
    double x3 = cz    / d;
    double x4 = (d-1) / d;
    //Generalized Hilbert transform in conformal space
    double a  = pow(x1,2)+pow(x2,2)+pow(x3,2)+pow(x4,2);
    double pf = pow(pow(Fine  ,2) + a,-2.5);
    double pc = pow(pow(Coarse,2) + a,-2.5);
    double f  = Image3D(x + cx,y + cy,z + cz);
    double c  = f * (pf - pc);
    rp += f * (Fine*pf - Coarse*pc);
    r1 += x1 * c; r2 += x2 * c; r3 += x3 * c; r4 += x4 * c;
```

```
}
Curvature = atan(r2/r1);
Direction1 = asin(sqrt(pow(r1,2)+pow(r2,2))/r4);
Direction2 = atan2(sqrt(pow(r1,2)+pow(r2,2)+pow(r3,2)),r4);
Phase = atan2(sqrt(pow(r1,2)+pow(r2,2)+pow(r3,2)+pow(r4,2)),rp);
//For energy a DC free convolution kernel must be used instead
Energy = pow(rp,2)+pow(r1,2)+pow(r2,2)+pow(r3,2)+pow(r4,2);
```

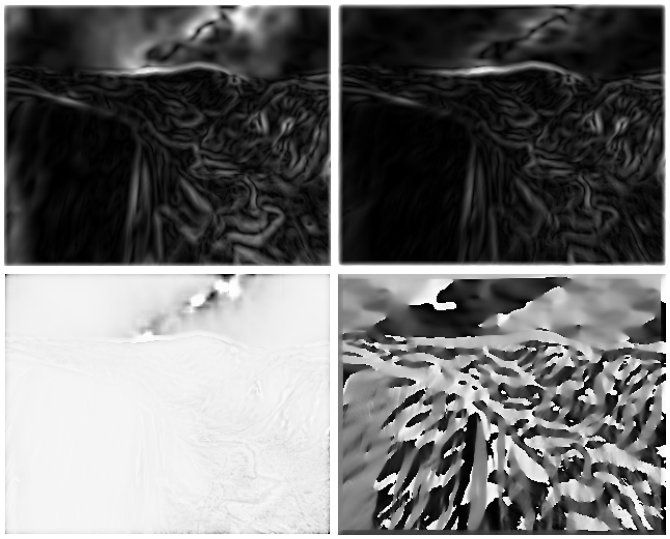

Fig. 6. The 3D *conformal monogenic signal* delivers four local features which can be used for image sequence analysis such as optical flow and motion analysis. First row shows from left to right: Curvature and phase information. Second row: Two parts of the orientation information. 3D convolution mask size $5 \times 5 \times 5$ pixels.

4 Conclusion

In this book chapter a new fundamental idea for locally analyzing 2D curved signals such as lines, edges, corners, arcs and circles in one unified framework has been presented. It has been shown that the feature space of the nth-order 2D Riesz transform is much too flat for analyzing 2D signals and extracting real i2D phase information. Generalized Hilbert transforms in Euclidean space lack from the restriction to the classical 1D phase information for all 2D signals. In such a case arbitrary 2D signals can be modeled by a superposition of individual i1D signals. The resulting system of equations to separate these i1D signals can not be solved in the most general case. The two-dimensional Riesz transforms of any order are always limited to the related 2D Radon

space which gives direct access to the feature space. To extend the dimension of the related feature space to analyze i1D and i2D signals in one framework, this problem can be solved by embedding 2D signals in higher dimensional conformal spaces in which the original 2D signal can be analyzed by generalized Hilbert transforms with more degrees of freedom. Without steering and in a rotationally invariant way, local signal features such as energy, phase, orientation/direction and curvature can be determined in spatial domain by 2D convolution. The *conformal monogenic signal* can be computed efficiently and can be easily implemented into existing low level image processing steps of Computer Vision applications. Furthermore, exact curvature can be calculated with all the advantages of rotationally invariant local phase based approaches (robustness against brightness and contrast changes) and without the need of any partial derivatives. Hence, lots of numerical problems of partial derivatives on discrete grids can be avoided. All results can be proved mathematically as well as by experiments. More applications of the *conformal monogenic signal* such as object tracking [14] on three-dimensional data will be part of our future work. The *conformal monogenic signal* shows the direct relation of the original image domain and geometric entities such as lines, circles, planes and spheres. For further results the reader is advised to have a look on our website `http://www.ks.informatik.uni-kiel.de/`.

References

1. S. Axler, P. Bourdon, and W. Ramey. *Harmonic Function Theory (Graduate Texts in Mathematics)*, volume 137. Springer, 2002.
2. S. Bernstein. Inverse Probleme. Technical report, TU Bergakademie Freiberg, 2007.
3. F. Brackx, B. De Knock, and H. De Schepper. Generalized multidimensional Hilbert transforms in Clifford analysis. *International Journal of Mathematics and Mathematical Sciences*, 2006.
4. R. Delanghe. Clifford analysis: History and perspective. *Computational Methods and Function Theory*, 1(1):107–153, 2001.
5. M. P. do Carmo. *Differential Geometry of Curves and Surfaces*. Prentice-Hall, 1976.
6. M. Felsberg. Low-level Image Processing with the Structure Multivector. Technical Report 2016, Kiel University, Department of Computer Science, 2002.
7. M. Felsberg and G. Sommer. The monogenic scale-space: A unifying approach to phase-based image processing in scale-space. *Journal of Mathematical Imaging and Vision*, 21:5–26, 2004.
8. V. Grau, H. Becher, and J. Alison Noble. Registration of multiview real-time 3-D echocardiographic sequences. In *MICCAI (1)*, pages 612–619, 2006.
9. K. Gürlebeck, K. Habetha, and W. Sprössig. *Funktionentheorie in der Ebene und im Raum (Grundstudium Mathematik)*. Birkhäuser, Basel, 2006.
10. S. L. Hahn. *Hilbert Transforms in Signal Processing*. Artech House Inc, Boston, London, 1996.

11. P. Kovesi. Phase congruency detects corners and edges. In *The Australian Pattern Recognition Society Conference*, pages 309–318, 2003.
12. P. Kovesi and A. Videre. Image features from phase congruency. *Journal of Computer Vision Research*, 1(3), 1999.
13. M. Krause and G. Sommer. A 3D isotropic quadrature filter for motion estimation problems. In *Proc. Visual Communications and Image Processing, Beijing, China*, volume 5960, pages 1295–1306. The International Society for Optical Engineering, Bellingham, 2005.
14. J. Lichtenauer, E. A. Hendriks, and M. J. T. Reinders. Isophote properties as features for object detection. *CVPR (2)*, pages 649–654, 2005.
15. T. Needham. *Visual Complex Analysis*. Oxford University Press, Oxford, 1997.
16. D. Reisfeld. The constrained phase congruency feature detector: Simultaneous localization, classification and scale determination. 17(11):1161–1169, 1996.
17. P. Toft. *The Radon Transform - Theory and Implementation*. PhD thesis, Technical University of Denmark, 1996.
18. L. Wietzke, O. Fleischmann, and G. Sommer. 2D Image analysis by generalized Hilbert transforms in conformal space. In *ECCV (2)*, LNCS, pages 638–649. Springer-Verlag, Berlin, Heidelberg, New York, 2008.
19. L. Wietzke and G. Sommer. The Conformal Monogenic Signal. In Gerhard Rigoll, editor, *Pattern Recognition*, volume 5096 of *LNCS*, pages 527–536. Springer-Verlag, Berlin, Heidelberg, New York, 2008.
20. L. Wietzke, G. Sommer, C. Schmaltz, and J. Weickert. Differential geometry of monogenic signal representations. In G. Sommer, editor, *Robot Vision*, volume 4931 of *LNCS*, pages 454–465. Springer-Verlag, Berlin, Heidelberg, New York, 2008.
21. D. Zang and G. Sommer. Detecting intrinsically two-dimensional image structures using local phase. In K. Franke, K.-R. Müller, B. Nickolay, and R. Schäfer, editors, *Pattern Recognition, 28th DAGM Symposium*, volume 4174 of *Lecture Notes in Computer Science*, pages 222–231. Springer-Verlag, 2006.
22. D. Zang, L. Wietzke, C. Schmaltz, and G. Sommer. Dense optical flow estimation from the monogenic curvature tensor. In *Scale Space and Variational Methods*, volume 4485 of *LNCS*, pages 239–250. Springer-Verlag, Berlin, Heidelberg, New York, 2007.